1997MNRAS.287..472D

Mon. Not. R. Astron. Soc. **287,** 472–480 (1997)

Unveiling a connection between large-scale structures behind the southern Milky Way

H. Di Nella,[1,2] W. J. Couch,[3] Q. A. Parker[4] and G. Paturel[1]

[1] *Observatoire de Lyon, F69230 Saint-Genis Laval, France*
[2] *Max-Planck-Institut für Astronomie, Konigstuhl 17, D69117 Heidelberg, Germany*
[3] *School of Physics, University of New South Wales, Sydney, NSW 2052, Australia*
[4] *Anglo-Australian Observatory, Coonabarabran, NSW 2357, Australia*

Accepted 1997 January 17. Received 1997 January 17; in original form 1995 November 27

ABSTRACT

A redshift survey of galaxies located in the direction of the southern Milky Way has been carried out using the FLAIR multi-objects system on the 1.2-m UK Schmidt Telescope (UKST) at the Anglo-Australian Observatory in Australia. The galaxy sample was extracted from the LEDA and COSMOS data bases, but essentially by scanning by eye four plates of the UKST/SERC Survey in the region between the Centaurus complex and the Pavo–Indus (PI) wall.

The galaxies selected have high central surface brightnesses and are distributed evenly over the whole search area. The majority of the galaxies have apparent magnitudes in the range $11.5 < B_J < 17$. Redshifts were determined for 211 galaxies, with one additional object being found to be Galactic – a planetary nebula.

A highly significant density enhancement is found in the galaxy distribution at 5000 km s^{-1} or 67 Mpc ($H_0 = 75$ km s^{-1} Mpc^{-1}). This suggests that a connection exists between the Centaurus complex and the PI wall across the zone of avoidance (ZOA) associated with the Milky Way, and as such could be one of the larger structures in the nearby Universe.

Key words: catalogues – galaxies: distances and redshifts – large-scale structure of Universe.

1 INTRODUCTION

In previous studies we showed that the spatial distribution of the nearest concentrations of galaxies (in walls or superclusters) suggests they are physically connected (Di Nella & Paturel 1995), while lying in the same preferential plane: the 'hypergalactic' plane (Bottinelli et al. 1986; Paturel et al. 1988; Di Nella & Paturel 1994). To test this hypothesis of connections between the nearest large-scale structures, we have conducted redshift surveys in crucial test regions.

In a recent paper (Di Nella et al. 1996) we tested the region between the Pavo–Indus (PI) wall and the Perseus–Pisces (PP) chain, which appeared as a void of galaxies, and a discontinuity in the connection between concentrations of galaxies in the hypergalactic plane. No evidence was found for a connection between the PP chain and the PI wall, but a southern extension of the PP chain was discovered. The PP chain has now been shown to extend more than 150 Mpc ($H_0 = 75$ km s^{-1} Mpc^{-1}). This is consistent with our view that large-scale structures are even larger than has been previously thought.

In the present paper we survey another important region in the direction of the Zone of Avoidance (ZOA), produced by the Milky Way, between the Centaurus complex and PI wall.

Another reason for testing this region, largely obscured by the southern Milky Way, is that it is located near the direction of the velocity vector of the CMB anisotropy and of the Great Attractor (Lynden-Bell 1991). It is important to probe the ZOA, because unknown extragalactic features could be hidden by the obscuration layer of our Milky Way, which might prove relevant in explaining the dipole motion. This is manifested, for example, by the recent POTENT analysis by Kolatt, Dekel & Lahav (1995), in which they show that the gravitational acceleration at the Local Group position changes by 31° when the matter distribution from within $|b| < 20°$ is included, bringing it very close to the CMB dipole. If mass overdensities are visible as galaxy over-

© 1997 RAS

Downloaded from https://academic.oup.com/mnras/article/287/2/472/1031495 by guest on 20 August 2022

© Royal Astronomical Society • Provided by the NASA Astrophysics Data System

1997MNRAS.287..472D

densities (e.g. Dekel 1994), it is important to unveil the distribution of galaxies behind the southern Milky Way.

The paper is organized as follows. Section 2 describes the observations and the data reduction, and Section 3 presents the results. In Section 4 the results are discussed and our conclusions are drawn.

2 OBSERVATIONS

2.1 Construction of the sample

It is well known that the obscuration of the Milky Way increases the apparent magnitudes and reduces the apparent angular diameters of galaxies (cf. Cameron 1990). For this reason, galaxies which lie close to the Galactic plane fail to meet the criteria for inclusion in catalogues (e.g. Lauberts 1982), and only a few galaxies are known at low galactic latitudes (i.e., $|b| \lesssim 10°$).

In addition, there are the enormous numbers of foreground stars that frequently fall on the galaxy images and crowd the field of view. A separation of galaxy and star images cannot yet be done reliably by automated measuring machines such as COSMOS or APM below $|b| \lesssim 10°-15°$. Examination by eye is still the best technique, although surveys by eye are clearly both very trying and time-consuming, and may not be as objective.

Nevertheless, such a survey has been carried within our region of interest. The tools for this galaxy search are very simple. It comprises a viewer with the ability to magnify 50 times and the IIIa-J film copies of the ESO/SERC survey. The success of the procedure for identifying extragalactic objects at very low latitudes is very good in the present survey where, of the 296 candidates, only one was found to be a Galactic nebula. This search procedure is very similar to the one described in earlier works by R. Kraan-Korteweg (e.g. Kraan-Korteweg 1989, 1991, 1992a,b; Kraan-Korteweg & Woudt 1994). It will be briefly described here.

To obtain our sample, we first selected galaxies in the obscured region between Centaurus and Pavo–Indus. This region corresponds to the range $75° \leq hgl \leq 105°$ and $-10° \leq hgb \leq +10°$ in hypergalactic longitude and latitude respectively (see Di Nella & Paturel 1994 for hypergalactic coordinate definition). To help the reader, we recall this definition of the hypergalactic coordinate system. The hypergalactic plane is defined by its pole: $l_p = 52°$; $b_p = 16°$ in galactic coordinates. The origin of hypergalactic longitudes is arbitrarily defined as $l(\text{origin}) = l(\text{pole})$ and $b(\text{origin}) = b(\text{pole}) - 90°$. The Cartesian XYZ coordinates are

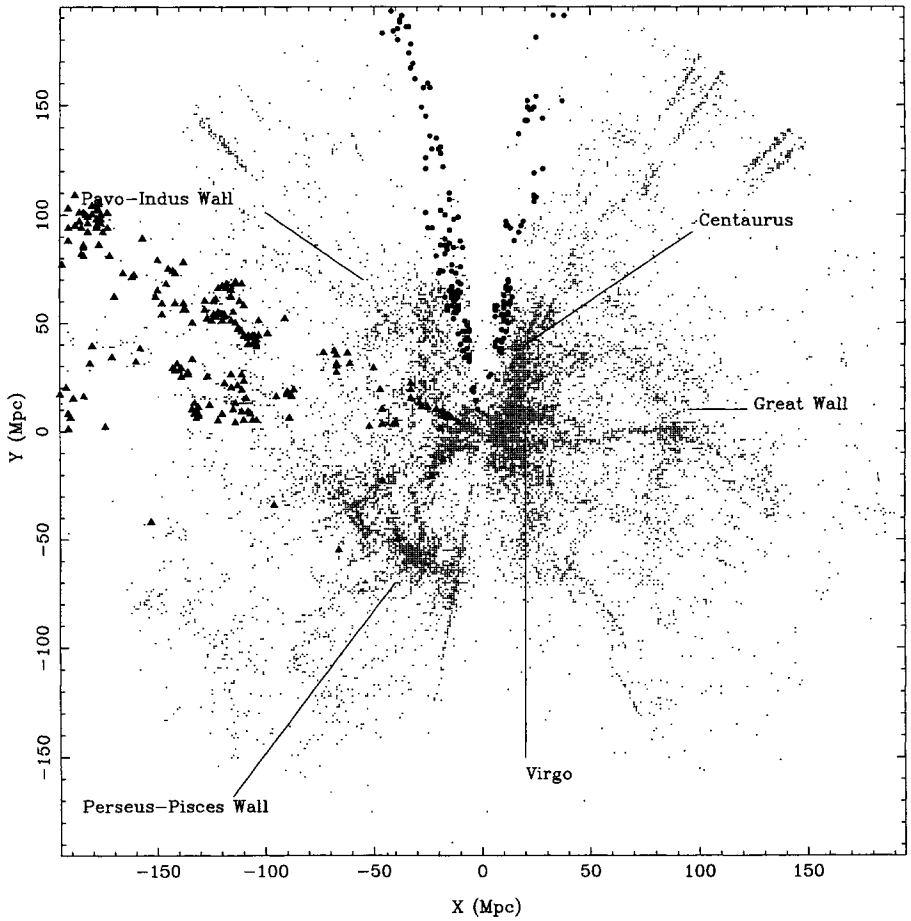

Figure 1. Distribution of galaxies in a face-on view of the hypergalactic plane. The filled circles represent LEDA galaxies previously measured in redshift, the triangles are the galaxies from the previous survey showing the southern extension to Perseus–Pisces (Di Nella et al. 1996), and the dots are from this survey. The density peak seen in the histogram of the velocities of this survey corresponds to the concentration of galaxies showing the tendency of the Centaurus complex and the Pavo–Indus wall to be connected.

© Royal Astronomical Society • Provided by the NASA Astrophysics Data System

Downloaded from https://academic.oup.com/mnras/article/287/2/472/1031495 by guest on 20 August 2022

1997MNRAS.287..472D

Table 1. Selection of the target galaxies.

B_T magnitude range	*hgb* range in deg	*hgl* range in deg	RA and DEC of field centre	*l* and *b*	UKST/SERC field number	number of target objects
11.5-17	[-7;-1]	[71;81]	17h06 -60deg	329 -11	138	83
11.5-17	[+12;+18]	[79;85]	15h36 -40deg	333 +13	329	66
11.5-17	[-5;+1]	[96;102]	16h08 -65deg	321 -9.5	100	84
11.5-17	[+1;+7]	[99;105]	14h00 -50deg	314 +11	221	63

thus calculated from hypergalactic longitude and latitude *hgl* and *hgb* respectively, using the following equations:

$$X = r\cos(hgb)\cos(hgl), \quad (1)$$

$$Y = r\cos(hgb)\sin(hgl), \quad (2)$$

$$X = r\sin(hgb), \quad (3)$$

where r is the distance deduced from the radial velocity and the Hubble constant. With the target of mapping the connections between large-scale structures in the hypergalactic plane (Di Nella et al. 1996), we decided to limit ourselves in hypergalactic latitude and study only the galaxies lying close to the hypergalactic plane. This would encompass FLAIR observations across four UKST/SERC survey fields centred at approximately $hgb = 0°$ (see Table 1). From the LEDA data base, which contains published data on known galaxies, we selected all galaxies with no measured redshift and which are positioned in one of the four UKST fields to be observed. We then selected objects classified as galaxies (but which frequently were double stars) in the COSMOS data base in the same region. No other selection criteria such as diameter limit or magnitude limit were applied to these LEDA and COSMOS subsamples.

After matching galaxies in the LEDA and COSMOS subsamples (see the method described in Di Nella et al. 1996, section 3), we obtained a total of 296 galaxies for redshift determination as shown in Table 1. Galaxies with published redshifts were also observed to derive our external error.

2.2 Observing procedure

The survey was undertaken using FLAIR, the multifibre spectroscopy system on the 1.2-m UK Schmidt Telescope (UKST) at Siding Spring Observatory, Coonabarabran, Australia. FLAIR is ideal for this survey as it combines a large field of view ($6° \times 6°$), a large multiplex advantage (73–92 objects simultaneously, depending on the FLAIR plateholder used), a very accurate system of positioning the fibres, allowing us to also measure some galaxies with stars superimposed on their images, and a sufficiently faint limiting magnitude ($B_T \leq 17$) to sample efficiently the volume of interest.

The observations, spread over six half-nights from 1995 April 4 to 11, with an extra backup night allocated on April 25, are detailed in Table 2. Unfortunately, the fourth night was lost due to poor weather. The typical seeing for the other nights was 2–4 arcsec. One field containing 65–85 galaxies was observed per night. Half-night exposures were sometimes not enough to obtain data of adequate signal-to-noise (S/N) ratio. In these cases we reobserved the field for another half-night.

The length of an individual FLAIR exposure is determined mainly by the cosmic ray event rate, typically 2–3 per minute. After 3000 s, ~ 100 cosmic ray events may be detected, resulting in significant clutter of a data frame. Important features in galaxy spectra may thus be compromised. Therefore an upper limit of 3000-s exposure was adopted. The typical total exposure time per field was in the range 3×3000 to 7×3000 s. 5×3000 s exposures are normally considered adequate to obtain spectra of S/N ratio ~ 20.

The G300B grating was used, giving 232 Å mm^{-1} or 5.12 Å pixel^{-1} (CCD resolution). The 2850-Å range provided at this dispersion was set around 4400–7360 Å.

To wavelength-calibrate the data, arc exposures were taken before and after a set of field exposures. The extremely stable nature of the floor-mounted FLAIR spectrograph obviates the need for more frequent calibration exposures (e.g. Parker & Watson 1995). Light from a selection of calibrating arc lamps was observed by reflection on the closed dome. Arc exposures were also taken when changing plateholders to account for the different fibre-formats, focus values, etc. Both neon and Hg–Cd arcs were combined to provide adequate line coverage over the observed wavelength range.

Table 2. Details of the observations.

ESO/SERC field #	Night of April 1995	Seeing arcsec.	Total expos. time sec.
100	4th/5th	2-3	17000
329	5th/6th	2	10600
221	7/8 + 8/9 + 25/26	2-3	21500
138	10th/11th	2-3	9000

Downloaded from https://academic.oup.com/mnras/article/287/2/472/1031495 by guest on 20 August 2022

© Royal Astronomical Society • Provided by the NASA Astrophysics Data System

1997MNRAS.287..472D

Flat-field exposures were taken using either the zenith twilight sky or by reflection on a dome flat-field screen of a featureless quartz-halogen lamp. These exposures were used to obtain the fibre-to-fibre transmission function (see Parker & Watson 1990) vital to ensure proper sky subtraction. Differences between fibre transmission efficiencies between the twilight sky and dome flats were at the ~ 2 per cent level (Parker & Lee 1994). Bias frames were also taken before and/or after observations. Among the available fibres, 5–8 were devoted to the night sky to facilitate satisfactory sky subtraction across the wide field.

The data reduction process is the same as the one we described in our previous paper (Di Nella et al. 1996). We used the NOAO IRAF spectral reduction package, together with a few additional FLAIR-specific IRAF tasks. A FLAIR IRAF data reduction manual exists to facilitate the process. It is based mainly on existing IRAF packages for multifibre spectroscopy such as 'DOHYDRA'. The final derivation of the radial velocities was done using the 'RVSAO' cross-correlation IRAF package.

2.3 Derivation of radial velocities

The reduced spectra from 'DOHYDRA' can be input to the IRAF 'RVSAO' task to derive the galaxy radial velocities via cross-correlation against filtered galaxy templates provided by Q. A. Parker. Such reduction procedures are described in detail by Parker & Watson (1990) and Watson et al. (1991).

We finally observed four sets of ~ 60–80 galaxies. Among the 296 galaxies observed, 211 gave reliable radial velocities according to a set of strict criteria: height of the correlation peak and match between velocities deduced from emission and absorption lines. An overall success rate of 71 per cent was achieved.

3 RESULTS

3.1 Redshift measurements

The radial velocity measurements for this set of 211 galaxies are given in Table 3, together with the most important associated COSMOS image parameters (position, diameter, axis ratio, apparent magnitude and position angle). The columns of Table 3 are arranged as follows.

Column 1. Right ascension in h, min, s, tenths for Equinox 1950.0.

Column 2. Declination in deg, arcmin and arcsec for Equinox 1950.0. Coordinates are from the COSMOS data base, except for a few cases where positions were taken from the LEDA data base.

Column 3. PGC/LEDA number (Paturel et al. 1989a,b).

Column 4. Alternative name in a given hierarchy according to LEDA data base: NGC, IC, ESO, MCG, FAIR and DRCG (Dreyer 1889–1910; Lauberts 1973–1982; Vorontsov–Velyaminov et al. 1962–1974; Fairall et al. 1990; Dressler 1980).

Column 5. Log of the major axis of the galaxy in 0.1 arcmin from the LEDA data base.

Column 6. Log of axis ratio from the LEDA data base.

Column 7. B_T magnitude from the LEDA data base.

Column 8. Heliocentric velocity from the literature (in km s^{-1}).

Column 9. Major axis in arcsec from the COSMOS data base.

Column 10. Minor axis in arcsec from the COSMOS data base.

Column 11. Position angle from the COSMOS data base. It is given in deg, measured from the north to the east.

Column 12. B_J magnitude from the COSMOS data base.

Column 13. Heliocentric velocity from this survey (in km s^{-1}).

Column 14. Notes.

3.2 COSMOS image parameters

The COSMOS image parameters listed in Table 3 were used to perform cross-identification with the PGC/LEDA objects, and are used in a companion paper (Rousseau et al. 1996) to convert diameters, axis ratios and magnitudes into the RC3 system (de Vaucouleurs et al. 1991).

3.3 Radial velocity external error estimates

To determine our external errors we have plotted in Fig. 2 the differences in velocity between our measurements and those of others as a function of our measured velocity. This comparison shows our measurements to be free of systematic or zero-point errors. The actual external mean error is computed to be $\sigma = 70$ km s^{-1}, if we assume that the velocities obtained from LEDA and the measurements of this survey have the same mean error.

4 DISCUSSION AND CONCLUSIONS

The aim of this survey was to study the distribution of galaxies in the region between the Centaurus complex and the PI wall, across the intersection between the hypergalactic plane and the southern Milky Way.

On the radial velocity histogram shown in Fig. 3, one can see evidence for a density enhancement at ~ 5000 km s^{-1}, which corresponds to both the velocity of the Centaurus complex and the PI wall. This seems to result from galaxies located in a connection between PI wall and Centaurus complex. In fact, we may consider the possibility of Centaurus being also directly connected to the Local Supercluster, which then must be much bigger than thought before.

ACKNOWLEDGMENTS

We are grateful to those who assisted during the observations at the UKST, and to those who manage the LEDA extragalactic data base. We acknowledge the COSMOS/UKST Southern Sky Catalogue supplied by the COSMOS group at the Royal Observatory Edinburgh to the Anglo-Australian Observatory. This work has been supported by grants from the Conseil Régional Rhone-Alpes (F) and by

Downloaded from https://academic.oup.com/mnras/article/287/2/472/1031495 by guest on 20 August 2022

© Royal Astronomical Society • Provided by the NASA Astrophysics Data System

1997MNRAS.287..472D

Table 3. The 211 measured galaxies.

RA 1950 DEC (1) (2)	PGC (3)	Name (4)	LEDA:logD (5)	logR (6)	bt (7)	Vleda (8)	a(") (9)	b(") (10)	PA (11)	BJmag (12)	Vsurvey (13)	
16 43 16.53 -60 03 31.5	PGC 0058999	ESO 137- 42	1.23	.35	13.59	3443					3180	
16 43 53.22 -62 35 31.2							30.9	17.9	93	14.96	4390	
16 46 07.21 -62 37 43.3											9620	
16 46 28.45 -61 39 36.5							17.9	16.0	85	15.39	4700	
16 46 39.61 -59 55 58.8							17.5	11.2	75	16.00	5870	
16 46 47.43 -58 54 26.5	PGC 0059112	NGC 6215	1.33	.05	11.93	1559	63.6	57.6	96	12.14	1500	
16 46 59.59 -59 09 00.2	PGC 0059124	ESO 138- 1	1.00	.30	14.27	2740	25.9	18.2	147	14.76	2700	
16 47 16.54 -61 28 57.4							27.1	13.5	119	15.37	4650	
16 47 23.23 -59 20 34.1							12.9	11.1	120	16.22	14200	:
16 48 15.45 -62 21 27.5	LEDA0090259	IRAS16482-6221				4989	16.2	13.7	153	15.77	4920	
16 48 27.23 -58 35 13.7							27.0	17.7	148	14.66	2440	
16 48 36.10 -59 36 43.5							19.8	14.8	152	15.72	14200	
16 49 17.93 -62 39 26.7							18.6	9.9	37	15.85	4380	
16 50 13.55 -59 56 50.9							15.5	12.1	162	15.82	13300	
16 51 37.70 -59 19 51.7							18.4	11.2	166	15.67	4760	
16 53 00.00 -62 45 45.0							14.3	11.2	158	16.35	14800	
16 54 19.60 -61 12 50.4							19.8	17.0	96	14.96	4960	
16 54 35.12 -60 08 30.7	PGC 0059373	ESO 138- 10	1.76	.14	11.57	1145	130.6	95.9	41	11.55	1070	
16 54 58.26 -62 28 17.9	PGC 0059389	ESO 138- 11	1.03	.22	14.18		32.7	19.4	175	14.13	4902	
16 55 02.56 -62 20 09.6							16.3	15.3	150	15.53	9300	
16 57 20.41 -60 34 41.5							20.4	7.0	104	16.16	4800	
16 58 11.77 -58 38 59.5							18.8	11.2	166	15.74	6340	
16 59 07.90 -58 00 35.2							18.0	8.2	119	16.26	14500	
17 02 23.40 -62 01 00.4	PGC 0059635	ESO 138- 14	1.64	.91	13.12	1507	140.9	15.4	136	13.19	1400	
17 02 33.93 -60 02 51.7							19.6	8.6	138	15.97	4250	
17 03 23.61 -60 24 49.1							12.1	8.3	120	16.33	14190	
17 04 42.64 -61 32 54.8							30.9	11.1	128	15.32	4210	
17 05 39.53 -61 51 17.8	PGC 0059737	ESO 138- 16	1.17	.43	14.08		36.1	16.9	126	14.31	4748	
17 09 23.39 -60 45 06.4	PGC 0059887	ESO 138- 18	1.03	.40	14.93		30.9	12.1	17	14.88	5000	
17 10 40.55 -61 19 27.6							27.5	13.8	71	14.88	7300	
17 14 00.66 -60 21 32.3							25.1	11.8	17	15.26	5710	
17 15 40.11 -60 06 22.0	PGC 0060092	ESO 138- 21	1.16	.26	13.94	4507	36.1	20.3	93	14.19	4500	
17 17 37.29 -60 17 12.3							16.3	15.3	43	15.53	14170	
17 18 13.46 -59 27 33.7	PGC 0060161	ESO 138- 22	1.13	.61	14.45		41.3	11.0	121	14.79	2639	
17 18 33.30 -61 50 28.4							18.6	14.8	90	15.39	7820	
17 18 55.59 -60 27 45.9							22.0	7.6	106	15.86	3500	
17 19 25.44 -59 57 07.2	PGC 0060208	IC 4646	1.50	.15	12.57	3174	82.5	55.4	21	12.34	3070	
17 19 41.20 -59 20 11.6	PGC 0060216	ESO 138- 24	1.38	.63	13.78	2860	43.0	15.4	62	14.32	2880	
17 21 56.86 -60 30 09.6							25.2	15.0	93	15.04	5770	
17 21 59.89 -59 41 06.0	PGC 0060290	IC 4652	1.10	.32	14.08		30.9	16.0	21	14.49	4020	
17 22 34.95 -60 50 13.3	PGC 0060311	IC 4653	1.20	.19	13.22	1905	46.4	28.3	46	13.71	1470	:
17 22 50.10 -61 58 02.5							29.2	22.4	106	14.66	4480	
17 23 08.96 -61 59 24.6							16.7	10.9	172	16.20	7320	
17 23 20.56 -61 19 05.7							20.4	12.4	41	15.47	4860	
17 24 42.95 -62 26 04.0	PGC 0060386	ESO 138- 3	1.15	.48	13.87		17.9	14.3	136	15.98	4800	
17 28 48.86 -60 44 28.1	PGC 0060487	ESO 139- 4	1.08	.32	14.57	5670	25.9	14.6	130	15.43	5730	
17 21 35.74 -59 43 35.9											6270	
17 25 49.58 -61 59 24.1	PGC 0060412	ESO 139- 1	.98	.11	14.20	4530	27.5	22.3	46	14.75	4400	
17 13 36.90 -59 07 06.0	PGC 0060029	NGC 6305	1.23	.20	13.19	2722					2650	
17 07 57.68 -61 02 41.7											16900	
17 04 23.26 -62 11 40.7							15.1	6.9	89	16.55	4260	
16 58 39.73 -62 20 24.7							17.0	7.7	113	16.68	1050	:
16 56 40.09 -62 07 43.6							13.6	9.8	1	16.54	13800	
16 56 25.91 -61 18 09.7							10.6	8.0	26	16.89	16620	
16 55 09.34 -58 41 43.5	PGC 0059399	ESO 138- 12	1.15	.19	14.09	4818					14630	!!id
16 53 21.00 -62 38 48.0	PGC 0059334	ESO 101- 20	1.28	.34	13.37	5845					5040	!!
16 40 53.72 -62 49 09.5							26.5	14.5	76	15.03	4430	
16 46 00.31 -61 44 09.2											4310	
16 47 43.04 -59 48 13.5											14240	
16 48 29.90 -58 51 54.0	PGC 0059180	NGC 6215A	1.17	.48	14.15	2894					2910	
16 49 35.00 -58 41 48.0	PGC 0059216	ESO 138- 5	1.24	.11	12.75	2920					2630	
16 43 08.00 -57 20 00.0	PGC 0058985	ESO 179- 13	1.51	.24		835					750	
17 25 18.89 -58 05 47.0							9.6	8.4	102	16.83	15250	
17 03 22.00 -59 47 06.0	PGC 0059659	ESO 138- 15	1.29	.95	15.10						4650	
15 47 12.20 -63 33 07.1							16.0	13.3	82	15.89	6650	
15 48 45.19 -67 26 24.5	PGC 0056316	ESO 100- 2	1.09	.37			17.0	10.9	51	15.89	10300	
15 54 09.20 -66 09 22.7							26.4	17.8	141	15.34	9750	
15 55 28.78 -66 14 12.8	PGC 0056627	IC 4584	1.24	.06		3730	15.3	13.8	66	15.78	3700	
15 55 33.04 -66 10 51.1	PGC 0056630	IC 4585	1.38	.52	13.01	3705	43.0	22.2	53	13.79	3754	
15 59 52.75 -63 33 43.8							20.9	6.9	121	16.38	7390	

© Royal Astronomical Society • Provided by the NASA Astrophysics Data System

Downloaded from https://academic.oup.com/mnras/article/287/2/472/1031495 by guest on 20 August 2022

1997MNRAS.287..472D

Table 3 – *continued*

RA 1950 (1)	DEC (2)	PGC (3)	Name (4)	LEDA:logD (5)	logR (6)	bt (7)	Vleda (8)	a(") (9)	b(") (10)	PA (11)	BJmag (12)	Vsurvey (13)	
16 00 49.88	-67 30 37.3							17.5	10.9	72	15.94	4990	
16 01 51.67	-63 38 46.3							17.6	10.2	170	16.05	8100	
16 07 33.71	-66 31 31.0							15.9	12.9	34	15.70	5580	
16 09 12.55	-63 16 49.3	PGC 0057544	ESO 100- 13	.94	.72			23.6	10.3	146	15.54	3200	
16 14 28.76	-63 08 34.5							21.2	20.2	59	15.08	5150	
16 14 52.21	-64 41 05.6	PGC 0057830	ESO 100- 19	1.02	.80			20.4	6.7	15	16.46	7600	:
16 15 33.50	-62 52 32.0							15.3	11.0	134	16.18	9855	
16 17 25.75	-63 26 53.1	PGC 0057939	ESO 100- 20	.84			5160	27.5	26.6	62	14.38	5274	
16 18 50.19	-65 53 00.2							17.2	15.3	109	15.94	16650	
16 20 08.73	-66 23 14.8							21.2	7.3	173	16.45	6500	
16 20 57.94	-65 02 47.2							17.3	8.4	161	16.48	10400	
16 21 23.38	-62 51 02.6							18.9	13.6	40	15.67	3532	
16 21 58.98	-63 05 30.1	PGC 0058129	ESO 100- 23	1.38	.30		3835	14.3	13.6	57	16.06	3900	
16 22 03.92	-66 28 41.3							23.8	22.0	159	15.17	6790	
16 22 25.06	-66 32 47.0							17.9	9.5	94	16.25	6450	
16 22 48.94	-65 18 00.5	PGC 0058203	ESO 100- 24	1.04	.33			23.5	14.0	14	15.19	7760	
16 23 04.57	-66 40 57.4	PGC 0058218	ESO 100- 25	1.24	.12		6549	15.0	10.1	85	16.39	5660	!!id
16 24 03.14	-67 20 57.8							19.7	14.1	138	15.91	14926	
16 24 14.29	-66 23 31.0	PGC 0058320	ESO 100- 26	.99	.51			24.8	14.0	42	15.30	6554	
16 25 25.75	-67 35 47.5							18.5	16.2	4	15.61	17950	
16 27 56.96	-64 43 36.0							19.1	16.4	105	15.37	4450	
16 28 54.00	-64 24 49.0	PGC 0058495	FAIR 479				8350	16.0	11.5	153	16.11	13600	!!
16 29 28.28	-67 12 28.0	PGC 0058533	ESO 100- 28	1.07	.59			21.2	11.6	154	15.57	4700	
16 29 59.26	-64 57 46.2							21.7	13.6	63	15.58	12395	
16 30 52.90	-66 22 27.4							12.6	11.4	92	16.09	16760	
16 35 29.73	-67 21 18.0	PGC 0058734	ESO 101- 7	1.07	.79	14.98		34.4	7.5	47	15.41	6650	
16 36 07.00	-66 30 00.0	PGC 0058752	ESO 101- 8	1.21	.92	15.13	5070					4900	
16 31 41.94	-65 54 13.3	PGC 0058597	ESO 101- 1	1.04	.30	14.65		23.0	16.5	168	15.05	4850	
16 33 06.73	-65 29 27.3							14.0	7.4	138	16.55	16000	
16 33 06.84	-64 42 45.3	PGC 0058642	ESO 101- 3	1.19	.65	14.51		17.6	10.5	49	15.94	4900	
16 29 31.02	-63 59 39.5											15801	
16 27 06.38	-63 39 07.5	PGC 0058445	ESO 100- 27	.99				7.2	5.4	102	17.97	4709	
16 28 28.02	-67 41 44.5							22.2	10.1	97	16.03	14250	
16 20 52.52	-62 31 26.2	PGC 0058089	ESO 100- 22	1.23	.27		4746					4850	
16 16 07.17	-67 05 08.0							12.9	10.1	29	16.71	17968	
16 19 28.53	-66 03 35.8							13.2	11.4	176	16.75	17600	
16 12 05.59	-62 33 56.9	PGC 0057688	ESO 100- 15	1.07	.84			12.5	7.8	120	16.85	9900	
16 11 47.27	-65 31 42.2	PGC 0057686	ESO 100- 14	1.14	.17		6493					6650	
16 07 09.00	-62 16 46.0											5760	
16 04 26.78	-62 37 26.0							17.0	8.0	19	16.53	8328	
16 01 54.58	-63 46 07.0	PGC 0057151	ESO 100- 9	.99	.68							3550	
16 37 00.60	-65 04 07.3											15439	
16 34 32.52	-65 09 50.3							10.6	9.0	149	16.83	14500	:
15 50 53.81	-66 56 17.1							14.1	9.0	42	17.04	9300	
15 46 50.90	-66 55 21.1							11.0	8.6	79	16.93	21500	
16 36 35.23	-64 31 50.5											12800	
16 35 12.70	-64 27 34.8							14.6	12.1	122	16.28	15800	
16 30 17.20	-64 44 38.0							11.1	9.3	62	16.68	11400	:
16 32 29.15	-64 02 36.3							14.8	11.6	130	16.27	12900	
16 23 10.84	-64 47 56.1							12.5	10.9	112	16.84	11064	
16 20 45.11	-64 51 57.3											9933	
16 15 43.44	-64 41 22.0							9.1	6.1	5	17.53	19456	
16 12 17.39	-64 08 08.8							10.6	9.0	109	16.90	12150	
16 11 39.38	-64 19 07.3							12.2	8.2	13	16.94	7092	
16 05 46.44	-64 34 40.3											12000	
15 53 48.02	-62 44 35.8							13.0	7.5	169	16.77	7460	
15 54 48.72	-65 59 23.5											6450	
16 05 12.63	-64 52 55.3							12.9	11.1	39	16.58	15050	
15 59 53.10	-62 22 01.0											3500	
16 01 33.50	-67 34 55.0	PGC 0057148	ESO 68- 16A	.83	.43			27.5	18.9	1	14.59	4800	
16 12 28.32	-67 55 01.8	PGC 0057738	ESO 69- 1	1.03	.13			41.3	25.8	132	13.97	3547	
15 47 56.38	-62 39 38.2	PGC 0056269	ESO 100- 1	1.09	.69			12.9	9.3	126	16.51	6450	
16 19 56.28	-64 35 54.4	PGC 0058039	ESO 100- 21	1.03	.81			17.1	5.6	7	16.86	12000	:
13 43 40.01	-50 10 47.7							13.3	13.1	159	16.13	3167	
13 44 00.40	-51 27 48.9							32.7	15.3	127	15.26	3900	
13 45 08.76	-50 10 38.4	PGC 0048963	ESO 221- 1	.84	.15	14.64		24.4	11.4	98	15.47	8210	
13 46 20.12	-48 37 01.4							29.2	18.7	4	14.84	3897	
13 47 15.18	-52 41 55.0	LEDA0087377	IRAS13472-5241				3821					3948	
13 48 16.04	-52 40 31.1	LEDA0087378	IRAS13482-5240				3972					3990	
13 49 05.53	-48 59 37.0	PGC 0049262	ESO 221- 15	1.06	.71	15.57		21.8	6.1	159	16.07	3348	
13 50 33.80	-48 37 10.5							17.0	10.9	146	16.14	11800	
13 53 34.78	-48 15 10.3	PGC 0049591	ESO 221- 18	1.02	.12	14.57		24.3	22.0	137	14.85	2964	:

© Royal Astronomical Society • Provided by the NASA Astrophysics Data System

Downloaded from https://academic.oup.com/mnras/article/287/2/472/1031495 by guest on 20 August 2022

1997MNRAS.287..472D

Table 3 – *continued*

RA 1950 (1)	DEC (2)	PGC (3)	Name (4)	LEDA:logD (5)	logR (6)	bt (7)	Vleda (8)	a(") (9)	b(") (10)	PA (11)	BJmag (12)	Vsurvey (13)	
14 01 56.95	-48 21 01.1							20.8	16.0	28	15.36	2850	
14 05 11.27	-47 44 00.7	PGC 0050448	ESO 221- 26	1.45	.19	12.05	1396	85.9	61.8	2	12.26	9300	:!!id
14 05 20.59	-48 59 51.4	PGC 0050467	ESO 221- 27	1.12	.48	13.98		46.4	15.2	41	14.25	3200	
14 08 53.47	-49 09 18.4	PGC 0050706	ESO 221- 32	1.33	.07	12.73	2904	56.7	53.2	4	12.91	2894	
14 11 16.06	-48 12 56.4							24.5	13.8	102	15.23	4542	
14 12 31.70	-47 24 32.5	PGC 0050955	ESO 271- 26	1.09	.23	14.45	4797	44.7	21.6	100	14.34	4800	:
14 12 33.17	-51 46 47.5	LEDA0090187	IRAS14125-5146				4458	18.0	14.7	90	15.50	4442	
14 12 42.67	-52 22 36.4	PGC 0050968	ESO 221- 35	1.14	.64	15.09		26.2	14.7	31	15.19	3231	:
14 12 49.89	-47 53 44.0	PGC 0050966	ESO 221- 34A	1.75	.26	12.57						4170	:
14 14 56.00	-47 46 48.0	PGC 0051087	ESO 221- 37	1.19	.11	13.12	4742					4494	
14 06 32.24	-48 05 41.6	PGC 0050539	ESO 221- 29	1.16	.89	16.21		19.3	5.7	119	16.52	4194	
14 04 22.00	-48 09 24.0	PGC 0050388	ESO 221- 25	1.14	.37	14.57	2998					2933	
14 03 32.10	-48 32 49.3											2881	
14 07 21.58	-51 56 56.2	PGC 0050618	ESO 221- 30	.99	.71	16.34		13.9	8.7	58	16.58	3202	
13 55 42.84	-52 05 32.2											4065	
13 55 39.57	-49 22 56.1							17.9	6.4	89	16.68	8300	
13 47 15.00	-52 24 48.0	PGC 0049121	ESO 221- 7	1.20	.22	14.63	3661					3653	
13 49 44.25	-51 37 17.9							8.7	7.3	100	17.47	14666	:
13 46 07.99	-51 55 05.0							12.6	8.6	56	16.71	9160	
13 49 13.68	-50 08 09.3							23.1	6.9	138	16.51	8200	
13 44 21.10	-50 39 42.0											8450	
13 42 33.00	-50 12 42.0	PGC 0048789	ESO 220- 37	1.03	.00	14.71	8233					8369	:
13 41 50.00	-49 44 00.0	PGC 0048739	ESO 220- 36	1.10	.79	15.64		34.4	9.1	29	15.65	3583	
13 55 13.00	-48 13 54.0	PGC 0049722	ESO 221- 20	1.20	.14	13.22		41.3	30.3	129	13.79	2780	
14 12 13.00	-47 36 54.0	PGC 0050935	ESO 221- 33	1.01	.22	15.30		32.7	21.4	66	14.65	4600	:
15 20 31.82	-41 43 13.0							12.4	8.9	174	16.44	11930	
15 20 38.31	-38 48 27.1							14.0	7.9	171	16.68	7600	
15 20 49.55	-40 34 42.7							15.1	6.6	174	16.88	4550	
15 21 02.90	-38 54 37.3	PGC 0055002	ESO 328- 50	1.02	.35			34.4	19.9	82	14.39	7474	
15 21 03.73	-37 56 47.0	PGC 0054999	ESO 328- 49	.99	.63			23.2	7.6	68	15.80	5210	
15 22 32.10	-41 27 49.7							13.1	12.5	113	16.31	11580	
15 22 38.08	-41 50 02.3	LEDA0090207	IRAS15226-4149				4853	21.5	20.5	158	15.32	4850	
15 22 57.71	-41 29 44.1							16.3	7.1	84	16.62	11530	
15 23 00.35	-41 22 41.7							21.5	19.8	89	15.15	4700	
15 23 13.08	-39 00 29.1							14.0	9.4	41	16.27	5104	
15 23 20.00	-38 16 29.2							19.2	15.3	82	15.88	11400	
15 24 12.84	-42 34 44.9											11560	
15 24 42.10	-40 10 49.8	PGC 0055164	ESO 329- 4	1.08	.38			29.2	13.7	107	15.02	5437	
15 25 12.73	-38 27 49.8							15.8	9.4	22	15.98	4301	
15 26 04.33	-42 43 09.7	PGC 0055228	ESO 274- 17	.91	.32	15.50						3158	
15 26 36.61	-40 12 43.8							16.8	9.7	70	16.16	5156	
15 26 52.49	-38 28 51.1	PGC 0055256	ESO 329- 7	1.29	.55	13.28	4645	55.0	18.0	172	14.02	4650	
15 27 48.16	-40 41 06.1							11.6	10.2	93	16.62	2062	
15 28 16.73	-37 50 17.1	PGC 0055306	ESO 329- 8	.93	.72			16.8	7.6	111	16.40	7300	
15 30 45.83	-38 57 07.6							13.8	6.9	117	16.99	5500	:
15 31 48.68	-41 18 46.6	PGC 0055508	ESO 329- 10	1.13	.93			20.0	6.6	132	16.56	11815	
15 31 50.19	-39 01 25.6							18.4	14.1	114	15.90	5280	
15 33 43.19	-42 24 23.4							15.4	13.9	105	16.01	4496	
15 34 14.43	-40 39 44.5							15.8	7.4	163	16.74	14166	
15 34 58.23	-39 18 27.7							22.1	15.6	99	15.52	11650	
15 43 26.11	-41 06 19.8							21.1	11.8	14	15.86	7552	
15 44 25.63	-38 10 36.6	PGC 0056052	ESO 329- 20	1.04	.53			20.2	8.5	161	16.42	7500	
15 45 12.82	-40 21 12.4							15.3	6.9	134	16.62	4415	
15 48 32.70	-39 59 08.0											1940	:
15 50 54.00	-38 41 54.0	PGC 0056333	ESO 330- 4	1.00	.04	14.73						4220	
15 26 19.32	-42 13 58.6	LEDA0096566	IRAS15263-4213									11120	
15 38 09.43	-41 21 55.0											10663	
15 42 35.95	-39 38 03.0							7.8	5.1	109	17.95	7500	
15 25 03.50	-38 54 43.0	PGC 0055185	ESO 329- 5	.97	.77		4642					4630	
15 36 13.00	-38 22 36.0	PGC 0055718	ESO 329- 12	1.14	.00	13.79	4316					3100	!!
15 21 10.48	-42 28 57.4	PGC 0055011	ESO 328- 51	.99	.63			20.6	10.3	141	15.80	11100	
15 31 47.80	-38 31 35.3	PGC 0055504	ESO 329- 9	.88	.11			24.1	16.2	14	15.20	4491	
15 42 08.00	-41 04 48.0	PGC 0055960	ESO 329- 17	.93	.54							7460	
15 43 21.00	-42 11 12.0	PGC 0056015	ESO 329- 19	.93	.10							4490	
15 25 53.45	-39 04 53.8	PGC 0055212	ESO 329- 6	1.04	.07			21.4	10.7	123	16.07	6900	
15 28 16.03	-40 01 03.0							19.1	9.6	95	15.91	4240	
15 21 50.54	-40 14 36.2							12.7	9.7	135	16.78	14924	
15 46 16.00	-40 10 30.0	PGC 0056137	ESO 329- 22	1.19	.32		4445					4472	

Note: the ':' in the notes column indicates a poor determination of the redshift, the '!!' indicates a conflictual measurement against a previous one, and the 'id!!' indicates a conflictual identification.

© Royal Astronomical Society • Provided by the NASA Astrophysics Data System

Downloaded from https://academic.oup.com/mnras/article/287/2/472/1031495 by guest on 20 August 2022

1997MNRAS.287..472D

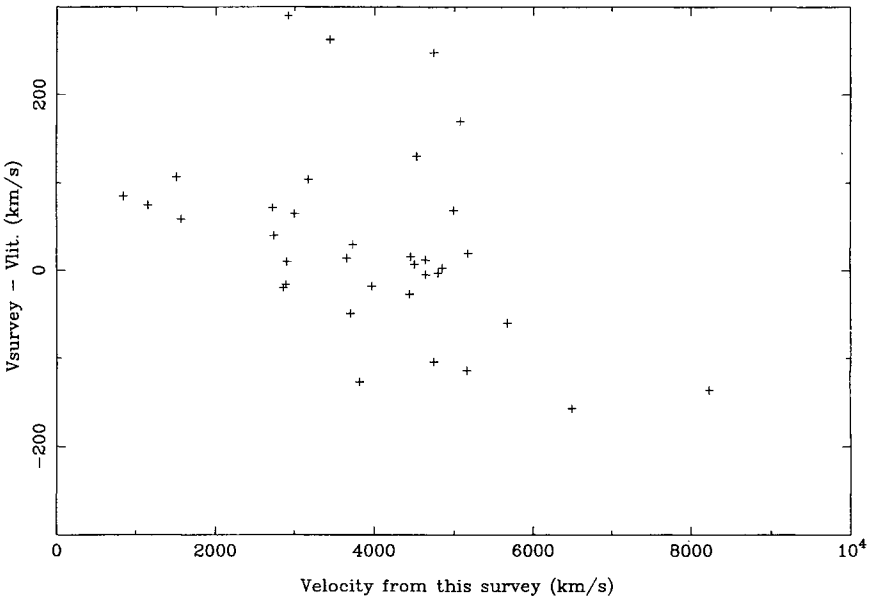

Figure 2. Comparison of new and published heliocentric velocities (see text).

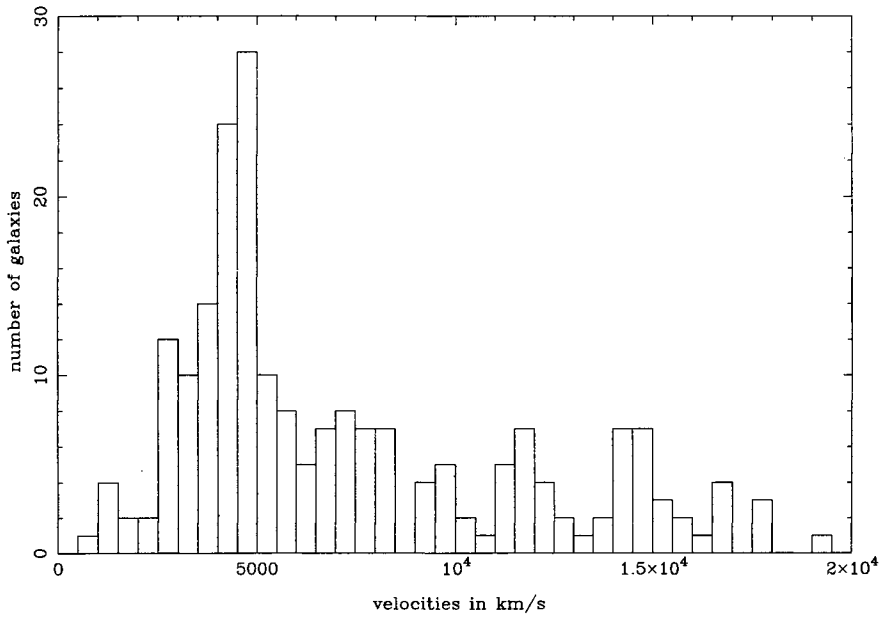

Figure 3. Histogram of radial velocities of the galaxies measured in this survey. A peak in density is seen at ~ 5000 km s^{-1}, which corresponds to the velocity of both the Centaurus complex and the Pavo–Indus wall.

the Institut National des Sciences de l'Univers (F) under the French–Australian cooperation scheme.

REFERENCES

Bottinelli L., Gouguenheim L., Fouqué P., Paturel G., 1986, in La Dynamique des Structures Gravitationnelles. Observatoire de Lyon, p. 95
Cameron L. M., 1990, A&A, 233, 16
Dekel A., 1994, ARA&A, 32, 371
de Vaucouleurs G., de Vaucouleurs A., Corwin H. G., Jr, Buta R. J., Paturel G., Fouqué P., 1991, Third Reference Catalogue of Bright Galaxies. Springer-Verlag (RC3)
Di Nella H., Paturel G., 1994, Comptes Rendus de l'Académie des Sciences Paris, Série II, t319, p. 57
Di Nella H., Paturel G., 1995, Publ. Astron. Soc. Aust., 12, 56
Di Nella H., Couch W. J., Paturel G., Parker Q. A., 1996, MNRAS, 283, 367
Dressler A., 1980, ApJS, 42, 565
Dreyer J. L. E., 1889, MNRAS, 49, 1 (NGC)
Dreyer J. L. E., 1910, MNRAS, 59, 105 (IC)
Fairall A. P., Palumbo G. G. C., Vettolani G., Kauffmann G., Jones A., Baiesi-Pillastrini G., 1990, MNRAS, 247, 21P
Kolatt T., Dekel A., Lahav O., 1995, MNRAS, 275, 797
Kraan-Korteweg R. C., 1989, Rev. Mod. Astron., 2, 119

Downloaded from https://academic.oup.com/mnras/article/287/2/472/1031495 by guest on 20 August 2022

© Royal Astronomical Society • Provided by the NASA Astrophysics Data System

1997MNRAS.287..472D

Kraan-Korteweg R. C., 1991, in Latham D. W., da Costa L. N., eds, ASP Conf. Ser. Vol. 15, Workshop on Large-Scale Structures and Peculiar Motions in the Universe. Astron. Soc. Pac., San Francisco, p. 165

Kraan-Korteweg R. C., 1992a, in Mamon G., Gerbal D., eds, 2nd DAEC Meeting on The Distribution of Matter in the Universe. Observatoire de Paris Press, Paris, p. 202

Kraan-Korteweg R. C., 1992b, in Warner B., ed., ASP Conf. Ser. Vol. 30, Variable Stars and Galaxies. Astron. Soc. Pac., San Francisco, p. 235

Kraan-Korteweg R. C., Woudt P., 1994, in Balkowski C., Kraan-Korteweg R. C., eds, ASP Conf. Ser. Vol. 67, 4th DAEC Meeting on Unveiling Large-Scale Structures behind the Milky Way. Astron. Soc. Pac., San Francisco, p. 99

Lauberts A., 1982, The ESO/Uppsala Survey of the ESO(B) Atlas, European Southern Observatory (ESO)

Lynden-Bell D., 1991, in Fabian A. C., ed., ASi Séries C, Vol. 366, Clusters and Superclusters. NATO, p. 241

Parker Q. A., Lee D., 1994, AAO Document on FLAIR Performance

Parker Q. A., Watson F. G., 1990, A&AS, 84, 455

Parker Q. A., Watson F. G., 1995, SPIE, Vol. 2476, 34

Paturel G., Bottinelli L., Gouguenheim L., Fouqué P., 1988, A&A, 189, 1

Paturel G., Fouqué P., Bottinelli L., Gouguenheim L., 1989a, A&AS, 80, 299

Paturel G., Fouqué P., Bottinelli L., Gouguenheim L., 1989b, Extragalactic Data Base Monographs 1, Vols 1, 2, 3 (PGC)

Rousseau J., Di Nella H., Paturel G., Petit C., MNRAS, 1996, 282, 144

Vorontsov-Velyaminov B. A., Arkipova V. P., Kranogorskaja A. A., 1962–1974, Morphological Catalogue of Galaxies. Trudy Sternberg Stat. Astron. Inst. 32, 33, 34, 38, 46

Watson F. G., Oates A. P., Shanks T., Hale-Sutton D., 1991, MNRAS, 253, 222

Downloaded from https://academic.oup.com/mnras/article/287/2/472/1031495 by guest on 20 August 2022

© Royal Astronomical Society • Provided by the NASA Astrophysics Data System